Service

Author Profile

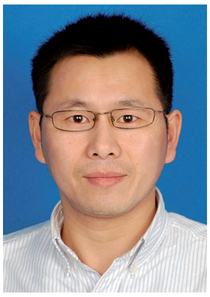

“My favorite food is huǒ guō (hotpot). The most exciting thing about my research is to make it after hundreds of failures ...”
This and more about Huisheng Peng can be found on page 918.

News

C. N. R. Rao

P. Jacobs

J. Sauer

Books

Highlights

Alkaloid Synthesis

X.-Y. Liu, D. Y.-K. Chen* ______ **924–926**

Synthesis of the C_{18}-Norditerpenoid Alkaloid Neofinaconitine: A Lesson in Convergent Synthesis Planning

Hexacyclic framework: The total synthesis of the complex C_{18}-norditerpenoid alkaloid neofinaconitine has been achieved by a convergent approach. This remarkable synthesis featured two Diels–Alder cycloadditions and subsequent Mannich-type *N*-acyliminium and radical cyclizations to establish the unique hexacyclic core structure of the target molecule.

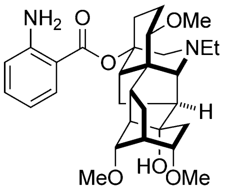

neofinaconitine

Natural Products

G. Appendino* ______ **927–929**

Omnia praeclara rara. The Quest for Ingenol Heats Up

Hit the mark: The development of a short synthesis of ingenol may mark the beginning of a new era of natural products synthesis, an era where structural complexity does not deter the development of processes amenable to scale up. This may foster the exploration of biologically relevant chemical space and pave the way to the development of commercial syntheses of natural products.

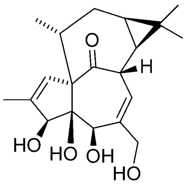

Ingenol

Materials Science

G. Qing, T. Sun* ______ **930–932**

Chirality-Driven Wettability Switching and Mass Transfer

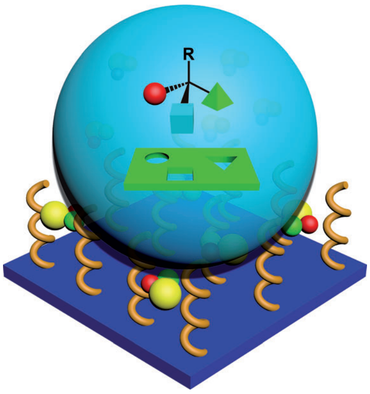

Enantioselective wetting: Regulating the surface wettability of materials through chiral molecules provides new insight into the design of chiral materials. By taking advantage of a reversible conformational transition, smart polymers present an ideal platform for translating weak chiral signals into macroscopic properties of materials, thus resulting in a distinctive wettability switching driven by chirality (see scheme).

For the USA and Canada:
ANGEWANDTE CHEMIE International Edition (ISSN 1433-7851) is published weekly by Wiley-VCH, PO Box 191161, 69451 Weinheim, Germany. Air freight and mailing in the USA by Publications Expediting Inc., 200 Meacham Ave., Elmont, NY 11003. Periodicals postage paid at Jamaica, NY 11431. US POSTMASTER: send address changes to *Angewandte Chemie*, Journal Customer Services, John Wiley & Sons Inc., 350 Main St., Malden, MA 02148-5020. Annual subscription price for institutions: US$ 11.738/10.206 (valid for print and electronic / print or electronic delivery); for individuals who are personal members of a national chemical society prices are available on request. Postage and handling charges included. All prices are subject to local VAT/sales tax.

Correspondence

Aniline Radical Cation

H.-G. Korth* ______ **934 – 937**

Comment on “Synthesis, Characterization, and Structures of a Persistent Aniline Radical Cation”: A New Interpretation Is Necessary

Further scrutiny for the aniline radical cation: The author of this Correspondence claims that the original spectrometric data for 2,4,6-tri-*tert*-butylaniline (TBA) reported in 2012 do not correspond to a stoichiometrically pure TBA$^{\bullet+}$SbF$_6^-$ salt, the quantum-chemical data do not support the reported structural data, and the interpretation of the apparent temperature-dependent structural changes in the solid state is open to interpretations other than the Jahn–Teller effect.

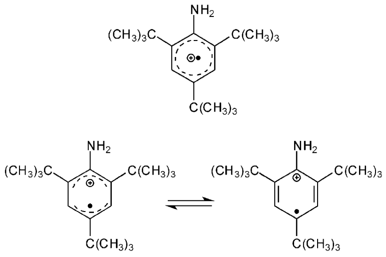

Aniline Radical Cation

M. R. Talipov, J. S. Hewage,
S. V. Lindeman, J. R. Gardinier,
R. Rathore* ______ **938 – 942**

Comment on “Synthesis, Characterization, and Structures of Persistent Aniline Radical Cation”: It Is a Protonated Aniline and Not an Aniline Radical Cation

The same, but different: The reaction of tri-*tert*-butylaniline (TBA) with AgSbF$_6$ in CH$_2$Cl$_2$ produces a green-colored intermediate which undergoes decomposition to form a protonated aniline (TBAH$^+$SbF$_6^-$). Crystals of the protonated aniline salt (see picture) were analyzed by X-ray diffraction and found to have the same crystal characteristics as the crystals of the supposed cation radical first identified in 2012.

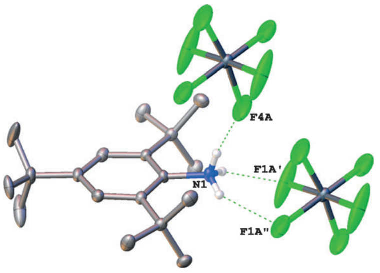

Aniline Radical Cation

X. Chen, X. Wang, Y. Sui, Y. Li, J. Ma,*
J. Zuo, X. Wang* ______ **943 – 945**

Reply to Comments on “Synthesis, Characterization, and Structures of Persistent Aniline Radical Cation”

The identification of the aniline radical cation TBA$^{\bullet+}$ (TBA = 2,4,6-tBu$_3$C$_6$H$_2$NH$_2$) reported in 2012 was questioned in the preceeding Correspondence articles. The original authors have reexamined their UV/Vis absorption and EPR data and insist that TBA$^{\bullet+}$ radical cation is indeed persistent and stable. The possible cocrystallization of TBA$^{\bullet+}$ with TBAH$^+$ makes crystal structures more complicated.

Minireviews

Surfactants

S. Polarz,* S. Landsmann,
A. Klaiber ______ **946 – 954**

Hybrid Surfactant Systems with Inorganic Constituents

Surf's up! Most surfactants are organic and contain a polar head group linked to a hydrophobic chain. However, the amphiphilic properties can be combined with the advanced functionality of transition-metal building blocks to give a new family of surfactants that have synergistic properties, and may lead to potential applications in catalysis, drug delivery, and smart materials.

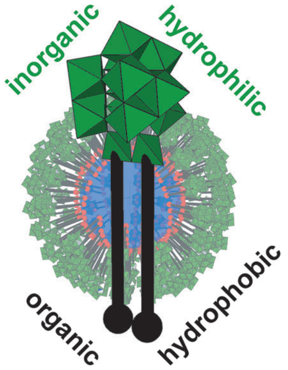

Highly attractive 2014 Rates*

for members of ChemPubSoc Europe societies

*(without local VAT)

ChemPubSoc Europe

IF 2012: 5.831

IF 2012: 3.344

IF 2012: 3.120

NEW to the family

Open-Access Journal

IF 2012: 3.740

IF 2012: 2.835

IF 2012: 7.475

IF 2012: 5.181

IF 2012: 3.349

New! Starting 2014

Online ordering:

Simply visit the journal's homepage at

www.onlinelibrary.wiley.com

Choose GET ACCESS Subscribe / Renew on the left-hand menu and complete your order.

SVENSKA KEMISTSAMFUNDET

KNCV

GDCh
GESELLSCHAFT DEUTSCHER CHEMIKER

Société Chimique de France

SCG Schweizerische Chemische Gesellschaft
SSC Société Suisse de Chimie
SCS Swiss Chemical Society

GÖCH
GESELLSCHAFT ÖSTERREICHISCHER CHEMIKER

MKE

SOCIEDADE PORTUGUESA DE QUÍMICA

Real Sociedad Española de Química

Association of Greek Chemists

www.chempubsoc.eu

PSJ-13-59145_gu

Reviews

Neurotrophin

J. Xu, M. H. Lacoske,
E. A. Theodorakis* ———— **956 – 987**

Neurotrophic Natural Products:
Chemistry and Biology

Touching a nerve: Neurotrophic natural products offer a promising therapeutic approach against various neurological disorders. This Review highlights the current synthetic strategies toward these compounds, summarizes their ability to induce neuronal growth, and discusses their potential in treating neurodegenerative diseases.

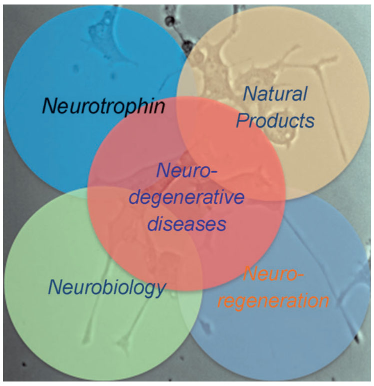

Front Cover

Communications

Affinity Pairs

L. Cao, M. Šekutor, P. Y. Zavalij,
K. Mlinarić-Majerski,* R. Glaser,*
L. Isaacs* ———— **988 – 993**

Cucurbit[7]uril·Guest Pair with an
Attomolar Dissociation Constant

A perfect pair: The complex between cucurbit[7]uril (CB[7]) and diamantane-4,9-bis(NMe$_3$) (**6**) has a dissociation constant of 1.4×10^{-18} M in aqueous solution. Competition experiments show that CB[7]·**6** is 143-fold stronger than the strongest CB[7]·guest complex measured previously.

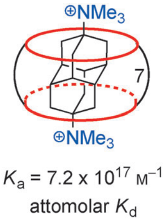

Frontispiece

G-Quadruplex Ligands

D. Verga, F. Hamon, F. Poyer,
S. Bombard,*
M.-P. Teulade-Fichou* ———— **994 – 998**

Photo-Cross-Linking Probes for Trapping
G-Quadruplex DNA

Catch me if you can: A readily accessible set of photoactivatable G-quadruplex (G4) ligands with a bisquinolinium core showed high G4-versus-duplex selectivity. Alkylation under UV/Vis irradiation occurred at G4 nucleobases located in either the loops or the external G-quartets (see picture), depending on the cross-linker and the topology of the quadruplex. These probes might be used to irreversibly trap G4 structures for the study of G4 biology.

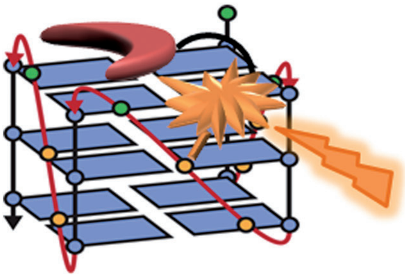

Quadruplex–Drug Complexes

W. J. Chung, B. Heddi, F. Hamon,
M.-P. Teulade-Fichou,*
A. T. Phan* ———— **999 – 1002**

Solution Structure of a G-quadruplex
Bound to the Bisquinolinium Compound
Phen-DC$_3$

Evidence stacks up for π-stacking: The structure of the complex formed between Phen-DC$_3$, which specifically targets G-quadruplexes and exhibits potent biological activity in vivo, and an intramolecular G-quadruplex derived from the *c-myc* promoter was solved by NMR spectroscopy. Phen-DC$_3$ was found to interact with the quadruplex through extensive π-stacking with guanine bases of the top G-tetrad (see picture).

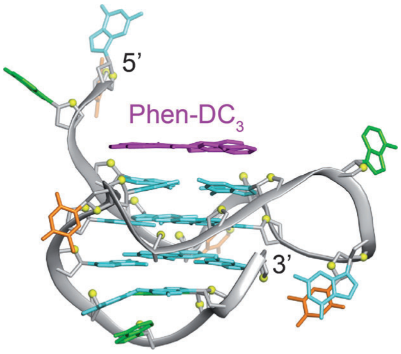

Molecular Recognition

Y. Jang, R. Natarajan,* Y. H. Ko,
K. Kim* ________________ 1003 – 1007

Cucurbit[7]uril: A High-Affinity Host for Encapsulation of Amino Saccharides and Supramolecular Stabilization of Their α-Anomers in Water

Sweet pockets: Cucurbit[7]uril binds protonated amino saccharides with excellent affinity in water. It stabilizes the α-anomers of the bound saccharides, thereby preventing any mutarotation in water, which is otherwise impossible. N blue, O red, H white.

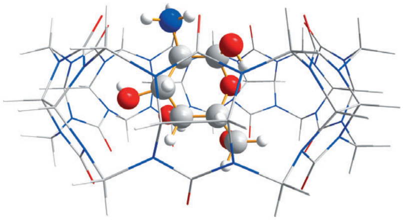

Molecular Imaging

H. Matsushita, S. Mizukami, F. Sugihara,
Y. Nakanishi, Y. Yoshioka,
K. Kikuchi* ________________ 1008 – 1011

Multifunctional Core–Shell Silica Nanoparticles for Highly Sensitive ^{19}F Magnetic Resonance Imaging

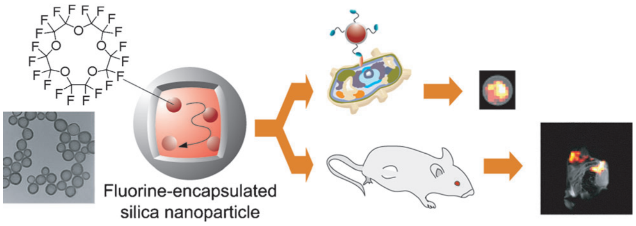

Highly sensitive ^{19}F magnetic resonance imaging (MRI) is a useful method for in vivo imaging without background signals. However, the low sensitivity of ^{19}F MRI limits its practical application. Novel multifunctional nanoparticles for highly sensitive ^{19}F MRI are reported, which consist of a liquid perfluorocarbon core and a silica shell (see picture).

Drug Design

Y. Min, J. Li, F. Liu, E. K. L. Yeow,*
B. Xing* ________________ 1012 – 1016

Near-Infrared Light-Mediated Photoactivation of a Platinum Antitumor Prodrug and Simultaneous Cellular Apoptosis Imaging by Upconversion-Luminescent Nanoparticles

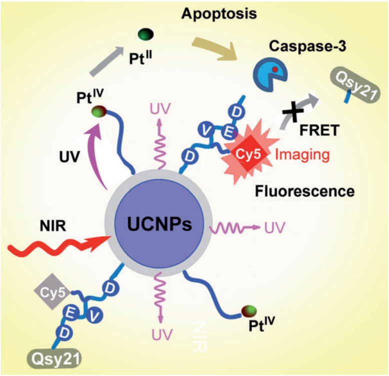

Platinum-based drugs: Near-infrared (NIR) light illumination of conjugates made of photoactive platinum(IV) prodrugs and upconversion-luminescent nanoparticles (UCNPs) is used for the remotely controlled activation of antitumor effects and for simultaneous initiation of apoptosis in the targeted tumor cells. The apoptosis-dependent caspase-3 enzyme offers the promising possibility of imaging apoptosis in real time.

Venom Peptides

C. I. Schroeder, L. D. Rash,* X. Vila-Farrés,
K. J. Rosengren, M. Mobli, G. F. King,
P. F. Alewood, D. J. Craik,
T. Durek* ________________ 1017 – 1020

Chemical Synthesis, 3D Structure, and ASIC Binding Site of the Toxin Mambalgin-2

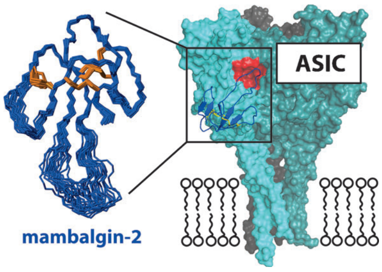

Toxic fingers pick ASIC's pocket: Efficient chemical synthesis of mambalgin-2 using native chemical ligation permitted the first structure determination of a member of this family of analgesic snake toxins. Electrophysiological analysis suggests that mambalgin-2, which was shown to adopt a three-finger toxin fold, binds near the acidic pocket on acid-sensing ion channels (ASICs).

Polycyclic Arenes

M. Bahou, Y.-J. Wu,*
Y.-P. Lee* ______ 1021 – 1024

Infrared Spectra of Protonated Coronene and Its Neutral Counterpart in Solid Parahydrogen: Implications for Unidentified Interstellar Infrared Emission Bands

Protonated pyrene and coronene collectively appear to have the required chromophores for the unidentified infrared (UIR) emission bands from interstellar objects, and the spectral shifts on an increase in the number of aromatic rings point in the correct direction towards the positions of the UIR bands. Larger protonated peri-condensed polycyclic aromatic hydrocarbons might thus be important species among the carriers of UIR bands.

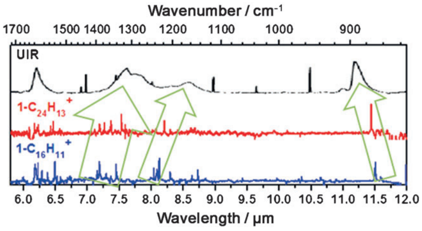

Protein Dynamics

L. Deshmukh, R. Ghirlando,
G. M. Clore* ______ 1025 – 1028

Investigation of the Structure and Dynamics of the Capsid–Spacer Peptide 1–Nucleocapsid Fragment of the HIV-1 Gag Polyprotein by Solution NMR Spectroscopy

HIV-1 Gag, a retroviral polyprotein that plays a central role in viral assembly, contains several domains of known structure. Solution NMR spectroscopy, including residual dipolar couplings, heteronuclear relaxation, and backbone chemical shifts, is used to probe the conformational dynamics of the 300-residue capsid (CA)–spacer peptide 1 (SP1)–nucleocapsid (NC) fragment of Gag, with and without nucleic acids.

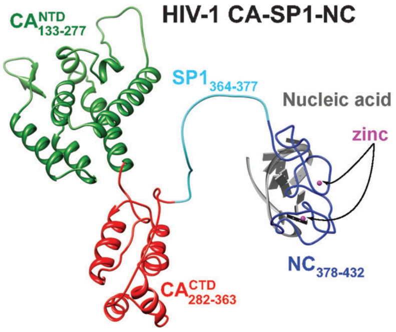

Photochemistry

S. H. C. Askes, A. Bahreman,
S. Bonnet* ______ 1029 – 1033

Activation of a Photodissociative Ruthenium Complex by Triplet–Triplet Annihilation Upconversion in Liposomes

Photoactivated chemotherapy: Liposomes capable of generating blue photons in situ by triplet—triplet annihilation based upconversion of either green or red light, were prepared. The liposomes were used to trigger the photodissociation of ruthenium polypyridyl complexes from ruthenium-functionalized PEGylated liposomes upon excitation with a PDT laser at 630 nm.

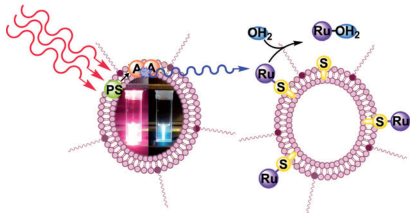

Zeolites

S. Wang, W. Yao, J. Lin, Z. Ding,
X. Wang* ______ 1034 – 1038

Cobalt Imidazolate Metal–Organic Frameworks Photosplit CO_2 under Mild Reaction Conditions

Inside Back Cover

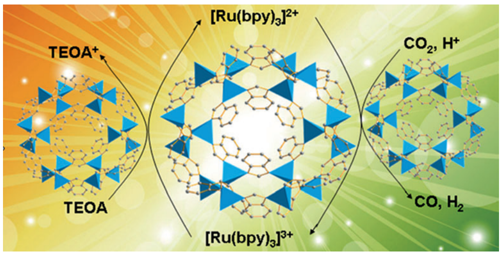

Splitting up: A cobalt-containing zeolitic imidazolate framework (Co-ZIF-9) has been used as a stable metal–organic framework cocatalyst with a photosensitizer to reduce CO_2. It combines benefits of the nanoporous characteristic of Co-ZIF-9 for CO_2 capture/activation and the catalytic redox function of cobalt centers. bpy = 2,2′-bipyridine, TEOA = triethanolamine.

Nonporous Sorbents

D. Solis-Ibarra,
H. I. Karunadasa* ________ **1039 – 1042**

Reversible and Irreversible Chemisorption in Nonporous-Crystalline Hybrids

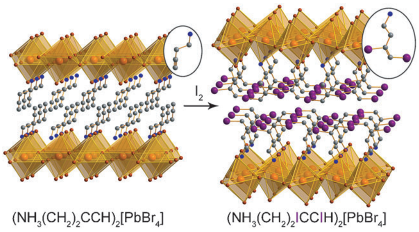

Sponges without holes: Alkyne groups in layered perovskites irreversibly capture I_2 vapor with high gravimetric and volumetric capacities, accompanied by volume increases of up to 36% with retention of crystallinity. Alkene groups in perovskites show reversible chemisorption of iodine to form diiodoalkanes, where the equilibrium for I_2 release can be tuned using packing effects.

Dynamic Porous Materials

A. Comotti, S. Bracco, T. Ben, S. Qiu,
P. Sozzani* ________ **1043 – 1047**

Molecular Rotors in Porous Organic Frameworks

Back Cover

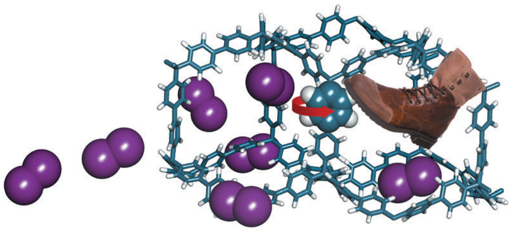

Fast molecular dynamics and large sorption capacity were combined in porous organic frameworks. The low-density, yet robust covalent architectures sustain extremely rapid rotational motion of the phenylene rings up to high temperatures. Porosity enables modulation of rotor dynamics by chemical stimuli: linear alkanes and iodine vapors, pervading the material, regulate rotor speed at will.

Supramolecular Chemistry

D. Xia, B. Wang, B. Chen, S. Wang,
B. Zhang, J. Ding,* L. Wang,* X. Jing,
F. Wang ________ **1048 – 1052**

Self-Host Blue-Emitting Iridium Dendrimer with Carbazole Dendrons: Nondoped Phosphorescent Organic Light-Emitting Diodes

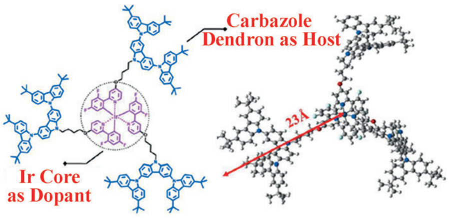

Out of the blue: The title dendrimer has been developed by covalently attaching a second-generation carbazole dendron to an emissive tris[2-(2,4-difluorophenyl)-pyridyl]iridium(III) core through a nonconjugated linker to form an efficient self-host system (see figure). Unlike small molecular phosphors and other phosphorescent dendrimers known to date, the nondoped phosphorescent organic light-emitting diodes herein are realized without a loss in efficiency.

Rare-Earth Complexes

K. Wang, G. Luo, J. Hong, X. Zhou,*
L. Weng, Y. Luo,* L. Zhang* **1053 – 1056**

Homometallic Rare-Earth Metal Phosphinidene Clusters: Synthesis and Reactivity

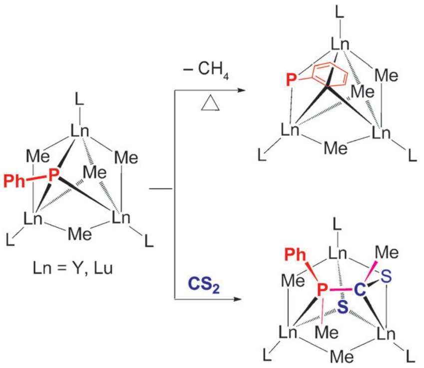

A rare gathering: Two new trinuclear μ$_3$-bridged rare-earth metal phosphinidene complexes were synthesized by treatment of the corresponding carbene precursors with phenylphosphine; some new transformation patterns of phosphinidenes are revealed. A possible pathway for reaction of these phosphinidene complexes with CS_2 was determined by DFT calculations.

Proteins

A. C. Obermeyer, J. B. Jarman,
C. Netirojjanakul, K. El Muslemany,
M. B. Francis* ____ **1057 – 1061**

Mild Bioconjugation Through the Oxidative Coupling of *ortho*-Aminophenols and Anilines with Ferricyanide

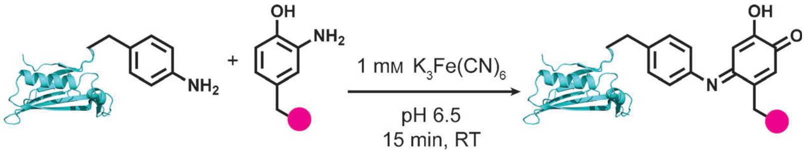

Having a complex: By using a small-molecule-based screen, ferricyanide was identified as an alternative, mild oxidant for the bioconjugation of anilines and *o*-aminophenols. The efficient coupling reaction is compatible with thiols and 1,2-diols, thus allowing its use in the creation of complex modified proteins.

Carbon Dispersant

D. Kuzmicz, S. Prescher, F. Polzer, S. Soll,
C. Seitz, M. Antonietti,
J. Yuan* ____ **1062 – 1066**

The Colloidal Stabilization of Carbon with Carbon: Carbon Nanobubbles as both Dispersant and Glue for Carbon Nanotubes

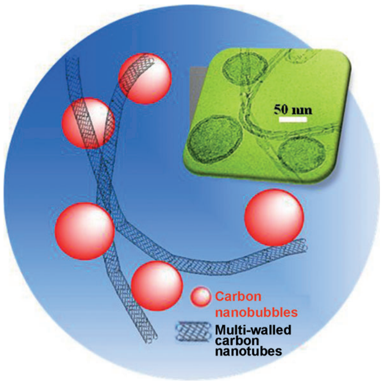

Tiny bubbles: A unique organic surfactant-free dispersion phenomenon of carbon nanostructures in aqueous solution is presented. Here, spontaneous Schottky charge transfer from carbon nanotubes (CNTs) to nitrogen-doped carbon "nano-bubbles" (CNBs) occurs, creating induced charges for effective stabilization. The interaction between CNTs and CNBs can be applied to create additive-free conductive carbon devices of various forms.

Trifluoromethylation

Y.-F. Wang, G. H. Lonca,
S. Chiba* ____ **1067 – 1071**

PhI(OAc)$_2$-Mediated Radical Trifluoromethylation of Vinyl Azides with Me$_3$SiCF$_3$

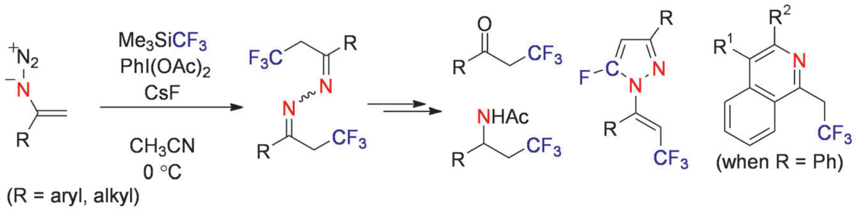

Trifluoromethylated diversity: The title reaction (see scheme) efficiently leads to α-trifluoromethyl azines, which were successfully transformed into valuable fluorine-containing molecules such as α-trifluoromethyl ketones, β-trifluoromethyl amines, 5-fluoropyrazoles, and trifluoroethyl isoquinolines.

Caged DNA

H. S. Steinert, F. Schäfer, H. R. A. Jonker,
A. Heckel,* H. Schwalbe* ____ **1072 – 1075**

Influence of the Absolute Configuration of NPE-Caged Cytosine on DNA Single Base Pair Stability

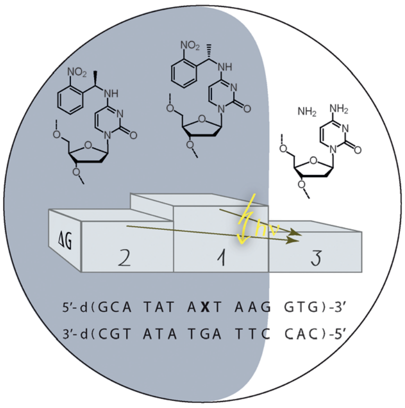

It's the stereo center: The (*o*-nitrophenyl)-ethyl caging group destabilizes duplex DNA. The effect depends on the absolute configuration of the stereocenter and is locally restricted. The structure models of the modified duplex DNA diastereomers reveal the distinct orientation of the caging group and provide the structural basis of the effect.

Enzyme Inhibitor

S. Mohan, P. S. Kerry, N. Bance,
M. Niikura, B. M. Pinto* ___ 1076 – 1080

Serendipitous Discovery of a Potent Influenza Virus A Neuraminidase Inhibitor

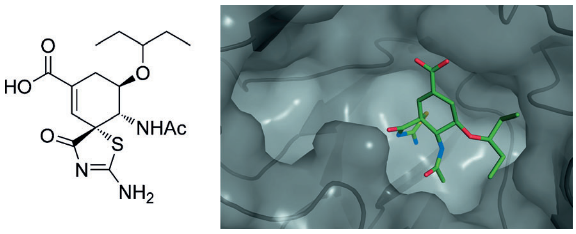

Serendipitous formation of a novel spirolactam affords a neuraminidase inhibitor, which inhibits replication of influenza virus A in cell culture. The X-ray crystal structure of the spirolactam in complex with the N8 subtype neuraminidase offers insight into the mode of inhibition.

H_2 Activation

W. H. Harman, T.-P. Lin,
J. C. Peters* ___ 1081 – 1086

A d^{10} Ni–(H_2) Adduct as an Intermediate in H—H Oxidative Addition across a Ni—B Bond

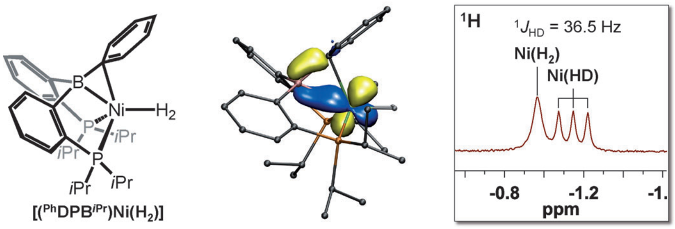

"B" for "better stability": NMR spectroscopy of the diphosphine–borane-supported Ni–(H_2) complex [($^{Ph}DPB^{iPr}$)Ni(H_2)] in solution confirmed the presence of an intact H_2 ligand (see picture). This nonclassical H_2 adduct is an intermediate in the cooperative activation of H_2 across the Ni—B bond. Electronic-structure calculations highlighted the important role of the borane ligand in stabilizing the Ni–(H_2) interaction.

Transition States

R. J. Williams, J. Iglesias-Fernández,
J. Stepper, A. Jackson, A. J. Thompson,
E. C. Lowe, J. M. White, H. J. Gilbert,
C. Rovira,* G. J. Davies,*
S. J. Williams* ___ 1087 – 1091

Combined Inhibitor Free-Energy Landscape and Structural Analysis Reports on the Mannosidase Conformational Coordinate

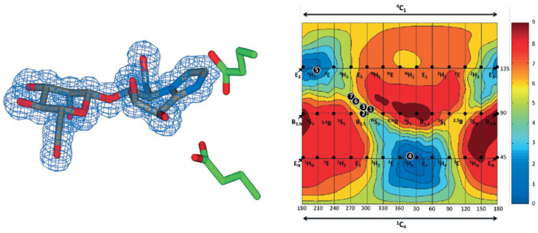

Shipshape inhibitors: Quantum mechanical calculations of the free-energy landscape (see figure) of the glycosidase transition-state mimics isofagomine and mannoimidazole reveals that only the latter is energetically poised to report upon the mannosidase transition-state conformation. X-ray structures of β-mannanases from different families reveal they both adopt a boat conformation, thus allowing unification of the enzymatic conformational itinerary of a range of diverse α- and β-mannosidases.

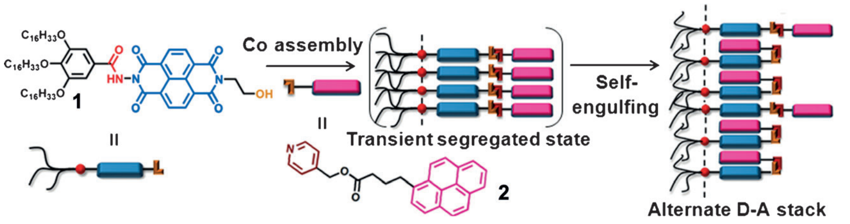

So many opportunities to get together: A naphthalene diimide building block **1** underwent self-assembly by orthogonal hydrogen bonding in a nonpolar solvent to form reverse vesicles, the temperature-dependent denaturation and redissolution of which led to reverse micelles. The coassembly of **1** with a pyrene donor **2** gave a transient donor–acceptor (D–A) complex, which formed an alternate D–A stack through a charge-transfer interaction (see picture).

Supramolecular Assembly

A. Das, S. Ghosh* ______ **1092 – 1097**

Stimuli-Responsive Self-Assembly of a Naphthalene Diimide by Orthogonal Hydrogen Bonding and Its Coassembly with a Pyrene Derivative by a Pseudo-Intramolecular Charge-Transfer Interaction

Inside Cover

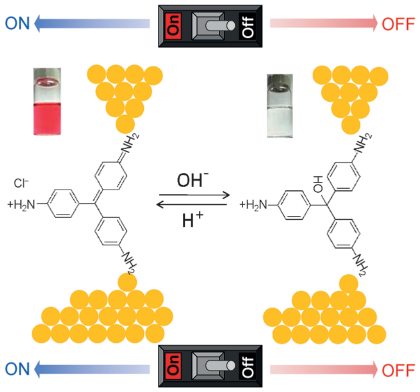

Molecular on/off switching: A single-molecule-based pH switch/sensor was fabricated exploiting the sensitivity of the dye molecules malachite green and pararosaniline (see picture). The high on/off ratio (ca. 100:1) of the device conductivity was confirmed by electron-transport calculations.

Single-Molecule Devices

Z. Li, M. Smeu, S. Afsari, Y. Xing, M. A. Ratner,* E. Borguet* _ **1098 – 1102**

Single-Molecule Sensing of Environmental pH—an STM Break Junction and NEGF-DFT Approach

---

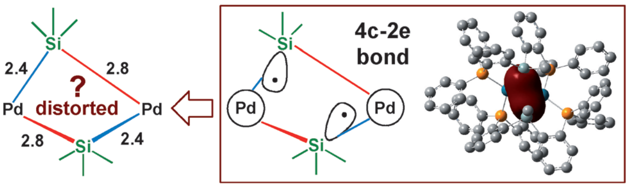

Strange to the core: In Pd and Ni dimers supported by PSiP ligands in which two hypervalent five-coordinate Si atoms bridge the two metal centers, a rare square-pyramidal geometry at Si and an unusual asymmetric M_2Si_2 core were observed. Natural bond orbital analysis showed that an asymmetric four-center two-electron (4c-2e) bond stabilizes the hypervalent Si atoms in the M_2Si_2 core (see picture).

Bonding Modes

A. Nova,* H.-W. Suh, T. J. Schmeier, L. M. Guard, O. Eisenstein, N. Hazari,* F. Maseras ______ **1103 – 1108**

An Unusual Example of Hypervalent Silicon: A Five-Coordinate Silyl Group Bridging Two Palladium or Nickel Centers through a Nonsymmetrical Four-Center Two-Electron Bond

---

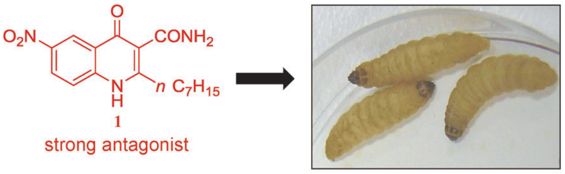

protects *Galleria mellonella* larvae

Jamming the talks for combating the bugs: The first PqsR antagonist that is potent in vivo and interrupts cell-to-cell communication in *P. aeruginosa* was discovered by overcoming an unexpected functional inversion that is mediated by a bacterial signal molecule synthase. The developed antagonist **1** protected *G. mellonella* larvae from bacterial infection at a very low dose.

Drug Discovery

C. Lu, C. K. Maurer, B. Kirsch, A. Steinbach,* R. W. Hartmann* ______ **1109 – 1112**

Overcoming the Unexpected Functional Inversion of a PqsR Antagonist in *Pseudomonas aeruginosa*: An In Vivo Potent Antivirulence Agent Targeting *pqs* Quorum Sensing

Drug Delivery

P. Moitra, K. Kumar, P. Kondaiah,
S. Bhattacharya* ________ 1113 – 1117

Efficacious Anticancer Drug Delivery Mediated by a pH-Sensitive Self-Assembly of a Conserved Tripeptide Derived from Tyrosine Kinase NGF Receptor

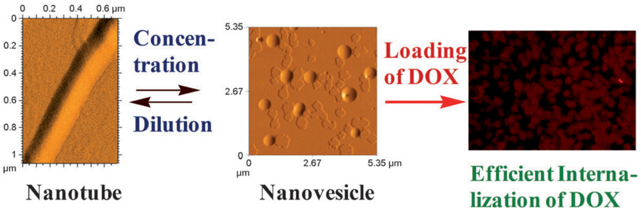

Package for special delivery: A biologically active tripeptide self-assembles to produce nanovesicles at lower concentrations and nanotubes at higher concentrations (see scheme). The nanovesicles rupture at pH ≈ 6 and are highly efficient in doxorubicin delivery to both drug-sensitive and drug-resistant cancer cells. This system is highly promising as a stimulus-responsive biocompatible nanovehicle.

Borane Carbonyl Derivatives

M. Sajid, G. Kehr, C. G. Daniliuc,
G. Erker* ________ 1118 – 1121

Formylborane Formation with Frustrated Lewis Pair Templates

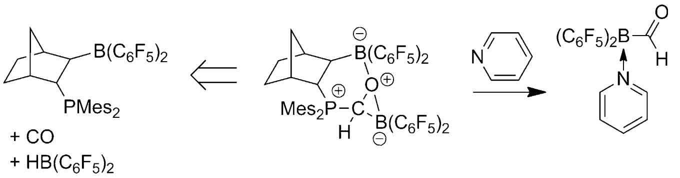

Channeling frustration into productivity: An elusive borane carbaldehyde was liberated from the product of carbon monoxide hydroboration at a frustrated Lewis pair template by treatment with pyridine and isolated as the donor-stabilized adduct (see scheme; Mes = mesityl). In this way, the thermodynamic restrictions of CO insertion into boron–hydrogen bonds could be circumvented.

Molecular Dynamics

T. Westermann, J. B. Kim,
M. L. Weichman, C. Hock, T. I. Yacovitch,
J. Palma, D. M. Neumark,
U. Manthe* ________ 1122 – 1126

Resonances in the Entrance Channel of the Elementary Chemical Reaction of Fluorine and Methane

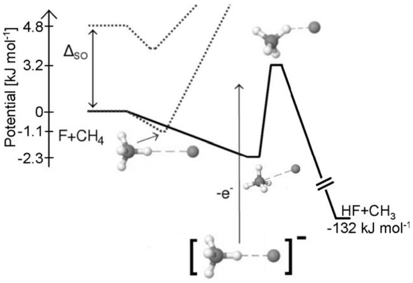

Chemical reactivity: Experimental and theoretical data consistently demonstrate the existence of resonances in the entrance channel of the $F + CH_4 \rightarrow HF + CH_3$ reaction shown by transition-state spectroscopy (see picture; Δ_{SO} = atomic spin–orbit splitting). Based on full-dimensional quantum dynamics simulations, a clear picture is drawn explaining the resonances.

Ligand Design

K. Fujimoto, T. Yoneda, H. Yorimitsu,*
A. Osuka* ________ 1127 – 1130

Synthesis and Catalytic Activities of Porphyrin-Based PCP Pincer Complexes

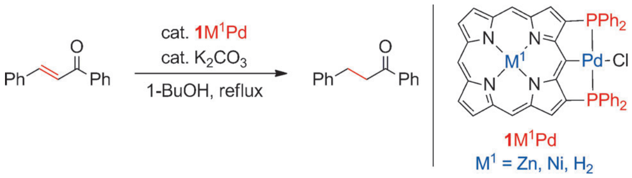

Metals at play: 2,18-Bis(diphenylphosphino)porphyrins undergo peripheral cyclometalation with group 10 transition-metal salts to afford the corresponding porphyrin-based PCP pincer complexes. The catalytic activities of the porphyrin-based pincer complexes were investigated in the allylation of benzaldehyde with allylstannane and in the 1,4-reduction of chalcone (see scheme) to assess the electronic interplay between the inner metal and the outer metal in catalysis.

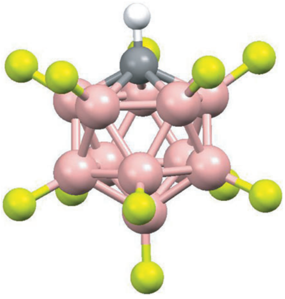

What’s eating you, alkane? The fluorinated carborane acid, $H(CHB_{11}F_{11})$, is shown to be the strongest Brønsted acid presently known. Remarkably, it protonates alkanes at room temperature. Stable carbocation salts are isolated. This novel superacid provides new opportunities to study the chemistry of hydrocarbon reforming.

The Strongest Acid

M. Nava, I. V. Stoyanova, S. Cummings, E. S. Stoyanov, C. A. Reed* **1131–1134**

The Strongest Brønsted Acid: Protonation of Alkanes by $H(CHB_{11}F_{11})$ at Room Temperature

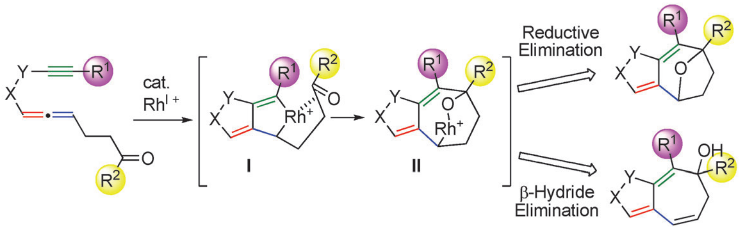

Unusual insertion: During the title reaction, a C=O bond is inserted into the $C(sp^2)$–Rh bond of rhodacycle intermediate **I**. The insertion occurs via a highly strained transition state. Direct reductive elimination from **II** gives a tricyclic product containing an 8-oxabicyclo[3.2.1]octane skeleton, whereas β-hydride elimination from **II** gives products with fused five- and seven-membered rings.

Cycloadditions

Y. Oonishi,* T. Yokoe, A. Hosotani, Y. Sato* **1135–1139**

Rhodium(I)-Catalyzed Cyclization of Allenynes with a Carbonyl Group through Unusual Insertion of a C=O Bond into a Rhodacycle Intermediate

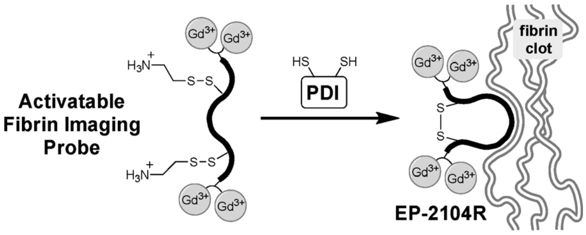

Identify new blood clots: The enzyme protein disulfide isomerase (PDI) plays an important role in facilitating the aggregation of activated platelets during the formation of new blood clots. By modifying a key disulfide bridge in the fibrin imaging probe EP-2104R, a new activatable magnetic resonance probe has been prepared that is responsive to PDI and therefore has the potential to be used for the identification of nascent blood clots.

Imaging Agents

G. S. Loving, P. Caravan* **1140–1143**

Activation and Retention: A Magnetic Resonance Probe for the Detection of Acute Thrombosis

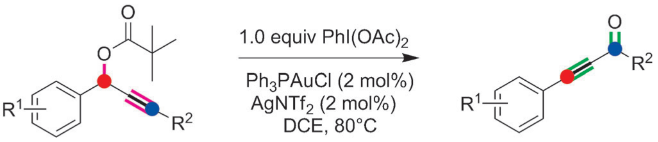

It takes alkynes: Propargyl esters can be converted into alkynyl ketones by a new oxidative gold-catalyzed reaction. The best catalyst system is $Ph_3PAuCl/AgNTf_2$ in combination with the oxidant $PhI(OAc)_2$. The yields are as high as 80% and the reaction can be conducted in the presence of air.

Homogeneous Gold Catalysis

Y. Yu, W. Yang, D. Pflästerer, A. S. K. Hashmi* **1144–1147**

Dehydrogenative Meyer–Schuster-Like Rearrangement: A Gold-Catalyzed Reaction Generating an Alkyne

Homogeneous Gold Catalysis

S. Shi, T. Wang, V. Weingand, M. Rudolph, A. S. K. Hashmi* ———— **1148 – 1151**

Gold(I)-Catalyzed Diastereoselective Hydroacylation of Terminal Alkynes with Glyoxals

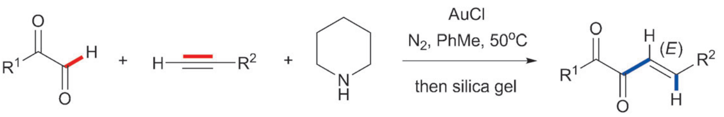

The simple AuCl catalyst and piperidine convert terminal alkynes and α-ketoaldehydes into 1,2-dicarbonyl-3-enes, the products of a formal hydroacylation of the triple bond, with excellent regio- and diastereoselectivity. There is no evidence for classical A^3 coupling products, which could be expected from such a gold-catalyzed reaction of an aldehyde, an amine, and a terminal alkyne.

Enantiomer Identification

V. A. Shubert, D. Schmitz, D. Patterson, J. M. Doyle, M. Schnell* ———— **1152 – 1155**

Identifying Enantiomers in Mixtures of Chiral Molecules with Broadband Microwave Spectroscopy

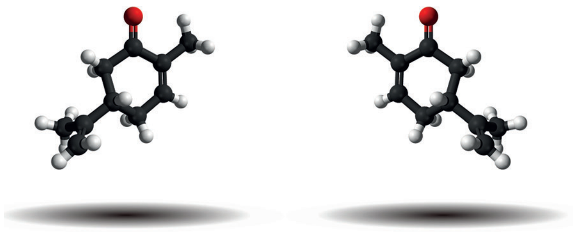

Enantiomer differentiation, enantiomeric excess measurement, and absolute configuration determination within a mixture of gas-phase chiral molecules are demonstrated. In these experiments, microwave three-wave mixing within supersonic jets is combined with chirped-pulse broadband microwave spectroscopy. This new technique is now a significant step closer to broader application.

Hydration Clusters

J. Thomas, O. Sukhorukov, W. Jäger, Y. Xu* ———— **1156 – 1159**

Direct Spectroscopic Detection of the Orientation of Free OH Groups in Methyl Lactate–(Water)$_{1,2}$ Clusters: Hydration of a Chiral Hydroxy Ester

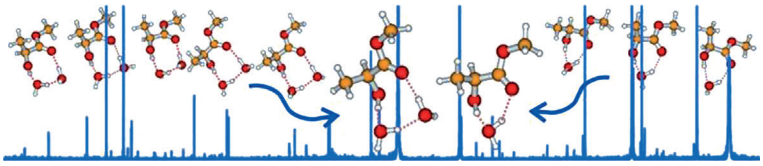

Small hydration clusters of methyl lactate show surprisingly specific binding preferences. They strongly prefer the insertion H-bonding topology, and favor specific orientation(s) for their non-H-bonded hydroxy group(s). Using a broadband chirped pulse and cavity based microwave spectroscopy, direct detection of such unique conformations of the methyl lactate–(water)$_{1,2}$ clusters is possible.

Carbohydrates

R. F. Martínez, Z. Liu, A. F. G. Glawar, A. Yoshihara, K. Izumori, G. W. J. Fleet, S. F. Jenkinson* ———— **1160 – 1162**

Short and Sweet: D-Glucose to L-Glucose and L-Glucuronic Acid

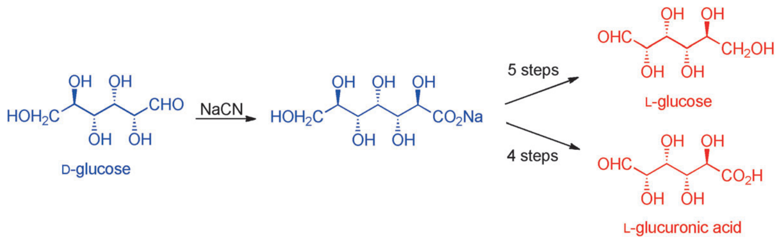

Short and sweet: The synthesis of 99.4% pure L-glucose and L-glucuronic acid from D-glucose via very inexpensive sodium glucoheptonate requires no purification of either intermediates or final products, other than extraction into and removal of solvents; a simple crystallization will raise the purity to > 99.8%. New diacetonides of glucose and glucuronolactone are reported.

Without N-protection: The oxidative addition of neutral 2-halogenoazoles to $[Pd(PPh_3)_4]$ followed by N-protonation provides access to palladium(II) complexes bearing protic NH,NH-functionalized NHC ligands (see example; NHC = N-heterocyclic carbene). The synthetic utility of the protic NH,NH-NHC ligands was demonstrated with their stepwise N,N′-alkylation.

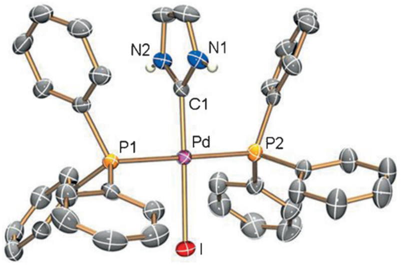

Protic N-Heterocyclic Carbenes

R. Das, C. G. Daniliuc,
F. E. Hahn* ———— **1163 – 1166**

Oxidative Addition of 2-Halogenoazoles—Direct Synthesis of Palladium(II) Complexes Bearing Protic NH,NH-Functionalized NHC Ligands

---

Supporting information is available on www.angewandte.org (see article for access details).

A video clip is available as Supporting Information on www.angewandte.org (see article for access details).

This article is available online free of charge (Open Access).

This article is accompanied by a cover picture (front or back cover, and inside or outside).

The Very Important Papers, marked VIP, have been rated unanimously as very important by the referees.

The Hot Papers are articles that the Editors have chosen on the basis of the referee reports to be of particular importance for an intensely studied area of research.

Angewandte Corrigendum

The authors of this Minireview have been made aware of a mistake in Scheme 4 and the corresponding text.[14] Compounds **35**–**38** which were described and drawn as *c*,*c*,*c*,*c*-[5.5.5.5]-fenestranes are in fact the *c*,*c*,*c*,*t*-[5.5.5.5] isomers. A corrected version of Scheme 4 is shown below.

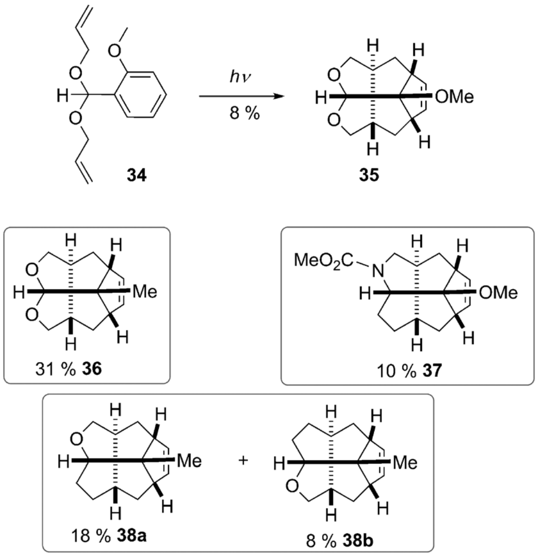

Scheme 4. Access to heterofenestranes through double arene–olefin cycloaddition.

Fenestranes in Synthesis: Unique and Highly Inspiring Scaffolds

A. Boudhar, M. Charpenay, G. Blond,
J. Suffert* ———— **12786–12798**

Angew. Chem. Int. Ed. **2013**, *52*

DOI: 10.1002/anie.201304555

Angewandte Corrigendum

Bis(amino)cyclopropenylidenes as Organocatalysts for Acyl Anion and Extended Umpolung Reactions

M. M. D. Wilde,
M. Gravel* ______ **12651–12654**

Angew. Chem. Int. Ed. **2013**, *52*

DOI: 10.1002/anie.201307167

In both reactions in Scheme 2 of this Communication, the reagent $NaBH_4$ must be replaced by $NaBPh_4$. The authors apologize for this oversight.